Experience with the Plate Structure of the Westinghouse Coil for the Large Coil Task

J. W. Lue, L. Dresner, M. S. Lubell, J. N. Luton, T. J. McManamy
Oak Ridge National Laboratory, Oak Ridge, TN USA

INTRODUCTION

The Large Coil Task (LCT) was a multinational cooperative research and development program to demonstrate the feasibility of building and operating large superconducting coils in a toroidal array similar to that required for a tokamak fusion reactor. Under the terms of an International Energy Agency (IEA) agreement, the United States (U.S.) built and operated the test facility at Oak Ridge, Tennessee, and provided three test coils. The other participants—EURATOM (EU), Japan (JA), and Switzerland (CH)—provided one coil each. Each coil was specified to have a D-shaped bore of 2.5 m by 3.5 m. Each was designed to produce 8.0 T at the reference point (innermost turn of the winding at the midplane of the coil width on the straight leg) when operating at its rated current in a six-coil array with the other five coils operating at 80% of their rated currents. The coils were subjected to 23 months of extensive testing with only one planned warmup to temperatures in the liquid nitrogen range. The test results were gratifying: each coil achieved design-point performance and beyond. A summary report was issued to make the LCT results and experience available to all potential users (Beard, 1988).

One of the U.S. coils was built by Westinghouse Electric Corporation (the WH coil). It had three unique features not seen in the other five coils: it was the only coil to use Nb_3Sn superconductor; its conductor was in a loose cable form rather than being a rigid monolith, as in the other coils; and it used aluminum alloy plates to provide a distributed coil structure rather than a lumped case structure. The performance of the Nb_3Sn superconductor and the stability of the cable-in-conduit conductor configuration were reported earlier (Dresner, 1987 and 1988). Here we describe test results related to the use of the aluminum plate structure.

COIL CONSTRUCTION

The completed WH coil (Singh, 1987b), shown in Fig. 1, was composed of 26 aluminum plates (including two outside dummies). The plates were made of 2219-T87 aluminum alloy, which had a yield strength of 454 MPa (65.8 ksi) and an ultimate tensile strength of 624 MPa (90.5 ksi) at 4 K. The coil was fabricated by bending and fitting square jacketed conductors into machined grooves in the structural plates, which were then bolted together with 570 throughbolts to provide a rigid structure. The plates were split near the horizontal midplane at three alternating locations to avoid large inductive loops. The finished coil pack had a radial build of 57 cm and an axial width of 75 cm at the midplane of the straight leg. Its 424 turns provided a total magnetomotive force of 7.53 MA-turns at the rated current of 17.76 kA. Conductors entered and left the support plates at the top of the coil to provide access for electrical and hydraulic connections.

*Research sponsored by the Office of Fusion Energy, U.S. Department of Energy, under contract DE-AC05-84OR21400 with Martin Marietta Energy Systems, Inc.

The conductor was composed of a cable with 486 fully transposed Nb_3Sn strands. The cable was encased in a 1.73-mm-thick stainless steel (JBK-75) sheath and compacted to 32% void. Six half-lapped layers of Kapton-H tape were wrapped on the 20.8- by 20.8-mm conductor to provide the insulating barrier from the grounded plates. No epoxy potting was applied between the conductor and the plate.

Aluminum rather than steel was chosen for the plate material to reduce weight and cost. The aluminum support structure was designed to fulfill two requirements: to carry the overall hoop and out-of-plane loads and to limit the transverse loading that the conductor had to carry. The loads were transferred from the conductor to the plates locally; thus, the conductor pack never had to carry its total cumulative load. This limited the conductor strains to a level that the Nb_3Sn and sheath material could tolerate.

The distributed structure provided not only local conductor support but also freedom of placement of conductors in the structure. The forces on the structure and conductor could be made uniform, and the accumulated force on the conductor and the structural support teeth could be made constant throughout the winding pack. This led to spiral grooves to accept two conductors at the inner turns, then four, and finally six conductors at the outer turns, as shown in Fig. 1. Because the distributed structure spreads the winding, this scheme also produces a higher on-axis toroidal field (for the plasma) for a given maximum field on the conductor (Singh, 1987a) than winding schemes that use lumped structure.

GENERAL TEST RESULTS

The coil was successfully charged to its rated current of 17.76 kA in both the single-coil mode and the six-coil full-array mode. In the full-array design-point test, the other five coils were charged to 88–96% of their rated currents to produce a uniform 8.0-T field at the reference point of each coil. In the extended single-coil test, the WH coil reached 131% of its rated current and a peak field of 8.2 T before it underwent a spontaneous quench, caused by unanticipated resistive heating in the conductor. In a second extended-condition test in single-coil mode, the coil was operated at temperatures higher than 4 K. The capability of the Nb_3Sn superconductor to operate at such higher temperatures was demonstrated by increasing the inlet helium temperature from the normal operating value of 3.8 K up to 8.0 K. The coil succeeded in reaching its rated current.

The extended-condition tests of WH coil in the full-array mode consisted of three series of charges to generate high fields. The first was a high-field torus test, in which the five background coils were charged to 88–97% of their rated currents; the WH coil reached 112% of its rated current and a reference field of 8.6 T. The other two tests were set up to achieve the same high field in each coil simultaneously. The second test demonstrated stable operation at fields of 8.4–8.5 T and coil currents of 94–107% of rated current. The last one ended in a spontaneous quench caused by resistive heating in WH coil. When the quench occurred, the peak fields in the six coils ranged from 9.0 to 9.2 T, and the stored energy of the array was 944 MJ—50% above the design value.

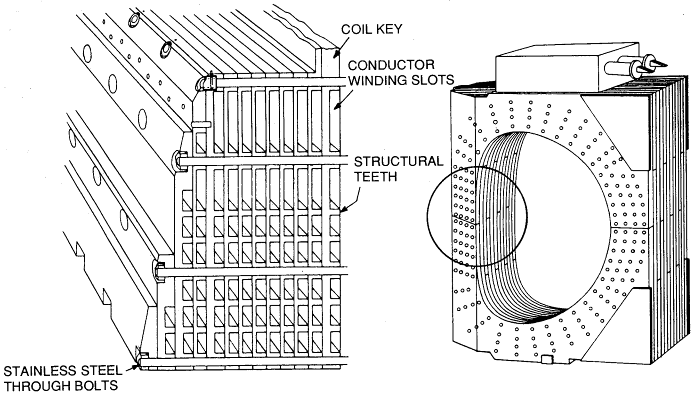

Over the course of the tests, the WH coil showed detectable resistive voltages above 70% of the rated current. Various specific measurements indicated that the Nb_3Sn was unexpectedly degraded, that the regions of degraded critical

Fig. 1. Schematic of WH coil showing the bolted plate structure.

properties were scattered throughout the coil, and that the resistive transition was broad. However, stability measurements showed that the coil could recover from an input heat density to the cable of 1.7–1.9 J/cm^3. Thus, despite the broad resistive transition, the stability margin of this cable-in-conduit conductor was still very high (Dresner, 1987 and 1988). Another gratifying result was that no helium leakage developed in the conductor or the insulation breaks.

MECHANICAL MEASUREMENTS

Single-Coil Charge

The coil was liberally supplied with strain gauges. The conductor jacket was equipped with 42 gauges, located on the four middle plates (plates 12–15), at the first two turns of the straight leg, at the top of the D, and at the outermost turn of the outer leg. Half of these gauges read longitudinal (hoop) strain; the other half read transverse (radial and axial) strain. In the rated current test, the only gauges that showed significant strain were those measuring longitudinal strain near the top and at the corner of the D. The largest strain recorded was 630 $\mu\epsilon$. Using an elastic modulus of 2.02 x 10^5 MPa, adopted by WH for the stainless steel jacket, yielded a stress of 125 MPa, far less than the stresses of 380 to 530 MPa predicted by WH. Since the coil tends to become round during a single-coil charge, the extended single-coil test produced the most severe bending stress on the winding. Again, the maximum strain was recorded near the point of largest curvature. The largest value was a hoop strain of 1750 $\mu\epsilon$. The maximum axial strain recorded was 600 $\mu\epsilon$; the maximum radial strain was only 300 $\mu\epsilon$, indicating that the compressive stress accumulation on the conductor was small in the plate-supporting scheme. Figure 2 shows the highest conductor hoop strains measured by the gauges in different test runs.

The structural plates were equipped with 60 additional strain gauges. Most were placed at locations similar to those of the conductor gauges, with additional gauges at the outboard region of the straight leg (the nose region) and a couple on each of the outside plates (i.e., plates 2 and 25). In the rated-current test, more strain gauges on the plates than on the conductor gave significant readings. The largest strains measured were the hoop strains in the outboard region of the curved outside leg. A maximum strain of 1100 $\mu\epsilon$ was measured. Using the elastic modulus of 7.7 x 10^4 MPa, adopted by WH for the aluminum alloy, we found a maximum stress of 83 MPa in the middle plates. This was again substantially less than the stresses of 140 to 190 MPa predicted by WH. Thus, it appeared that the cable itself carried substantial hoop loads, whereas the load sharing by the cable was assumed to be negligible in the calculation. In the extended single-coil charge, most strains were again roughly proportional to the current squared. Maximum hoop strains of about 2000–2200 $\mu\epsilon$ were recorded at the top of the D and the outboard of the outside leg. Figure 3 shows some hoop strains in the plates during different runs. Large radial strains of up to 1600 $\mu\epsilon$ (from the coil attempting to become round and pushing against the bucking post) were recorded at the nose region. Radial strains of less than 400 $\mu\epsilon$ were recorded at the outer leg. Figure 4 shows the compressive radial strain in the nose region and in the outer leg during different runs. The "bumps" in Figs. 2–4 were most likely due to stick-slip of the conductor.

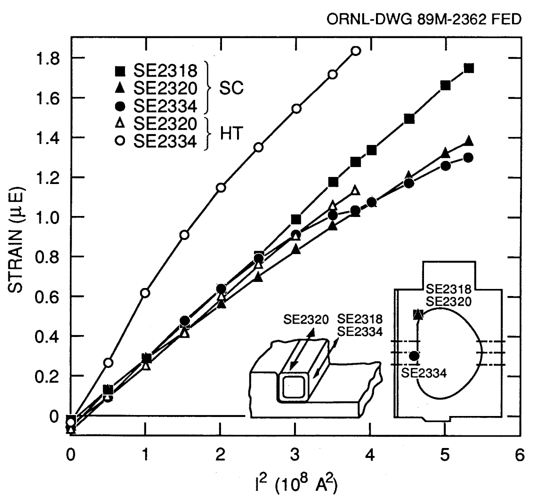

Fig. 2. Highest conductor hoop strains in extended single-coil (SC) and high-field torus (HT) tests. The much larger readings of gauge SE2334 at a given current in the high-field torus test were most likely due to the higher field at this location. Gauge SE2318 did not work during the high-field torus test.

Axial strains (due to radial stray fields that compressed the winding) of about 600 $\mu\epsilon$ were recorded at several locations.

Comparison of the strains on the conductor sheath and on the plate at the same location was inconclusive. However, the maximum strain on the conductor was about the same as that on the plate at similar locations. The conductor was only pressed into the grooves and not potted to the plate, so it probably contacted and transferred loads to the plate at discrete points. Thus, although the conductor and plate strains at a particular spot may not be the same, the global load transfer was effective.

<u>Full-Array Charge</u>

The 8-T design-point test was the charge mode for which the reduced-bending, D-shaped coils were designed. In such operation, however, the coils were subjected to large centering forces toward the bucking post. The 54-MN centering force on the WH coil produced a radial compressive strain of 1100 $\mu\epsilon$ at the nose region on the plate. The maximum hoop strains recorded on the conductor (850 $\mu\epsilon$) and on the plates (1200 $\mu\epsilon$) were very close to those for the single-coil run. They also occurred at the same places as in the single-coil test.

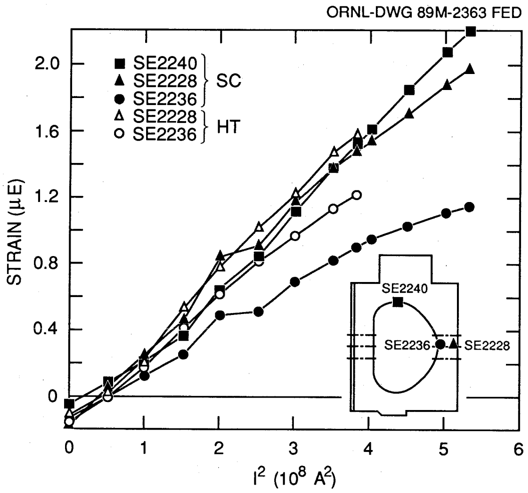

The largest strains experienced by the coil in full-array charge mode occurred in the high-field torus test. The largest conductor hoop strain was about 1800 $\mu\epsilon$, recorded at the inboard midplane of the straight leg. The maximum compressive strain on the plate at the nose region was 1600 $\mu\epsilon$, about the same as in the extended singlecoil test. The maximum hoop strain on the plate was 1600 $\mu\epsilon$. These results are also shown in Figs. 2-4.

Fig.3. Representative plate hoop strains in the extended single-coil (SC) and high-field torus (HT) tests.

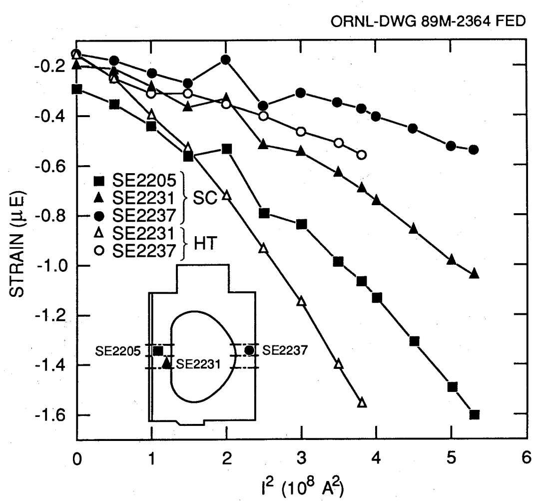

Fig. 4. Compressive strains in the nose region and the outer leg of the plates in extended single-coil (SC) and high-field torus (HT) tests. The much larger readings of gauge SE2231 at a given current in the high-field torus test were most likely due to the higher field at this location. Gauge SE2205 did not work during the high-field torus test.

Large Out-of-Plane Load Test

A possible failure mode in a toroidal array involves one de-energized coil while all the other coils are charged to high currents. In this case, the two coils on either side of the coil without current would be loaded with large out-of-plane forces, pulling them away from the coil without current. A test of this mode was conducted in conjunction with the CH coil by holding the EU coil at zero current. In this test, the WH coil was charged to 69.3% of its design current and was subjected to an out-of-plane load of 16.8 MN. Only moderate strains were recorded on the coil. The largest axial strain on the conductor (250 $\mu\epsilon$) was observed at the inboard midplane of the straight leg. Because of the test schedule, none of the strain gauges on the plates at the nose region (those that would most likely have registered large axial strains) was patched in for this test.

EFFECT OF PLATE SHORTING

As described earlier, to reduce the eddy currents caused by changes of magnetic flux, the aluminum plates were split and insulated by anodizing. During fabrication it was discovered that the plates had sharp edges at splits. The bolt holes had to be drilled and reamed, destroying the anodizing. Because the throughbolts were not insulated, the plates were shorted together and behaved electrically as an aluminum monolith.

A lumped-element circuit model was used to predict the coil response during a coil fast discharge (dump) (Luton, 1987). If there were full inductive coupling between the plate and the coil, the current in the coil would drop abruptly at the start of the dump by a factor of $\tau_2 /(\tau_1 + \tau_2)$, followed by an exponential decay with a time constant of $\tau_1 + \tau_2$. Also, the energy dissipation in the coil itself would be reduced by a factor of $\tau_2 /(\tau_1 + \tau_2)$. These predictions were verified experimentally. The self-inductance of the coil and the dump resistance in the circuit gave a primary time constant, τ_1 , of 7.2 s. The observed combined decay constant of 9.4 s implied a plate time constant, τ_2 , of 2.2 s. Thus $\tau_2 /(\tau_1 + \tau_2) = 0.77$; the coil current dropped by precisely this factor at the initiation of a dump.

A Rogowski coil placed on the outside leg of the coil over the plate stack and the embedded conductors did not show a sudden change in flux. The current represented by the 23% drop, amplified by the turns ratio of 424, had transferred inductively to the plates. At the coil rated current (of 17.76 kA), the peak eddy current induced in the plates was nearly 2 MA. This current did not seem to cause local hot spots in the plates or the bolt temperature sensors, indicating that, for the most part, the plate shorts were widespread and of low resistance. However, when the coil was inspected after completion of the tests, a spot of melted material was found between two plates near a bolt.

The energy deposited in the plates raised their temperature to about 45 K. Since the plates had no cooling channels, it took several hours to recool them. An analysis of recooling times and cooldown experience showed that the thermal coupling between the plates and the conductor was extremely poor. According to this analysis, the area of contact between the conductor and the plates was much smaller than the surface area of the conductor facing the plates. The conductor was energized to 10% of the rated current during recool to see if the Lorentz force would press the conductor against the plates and improve thermal contact. The recool time was reduced by up to 40%.

The substantial amount of stored energy (23% of the total) that was transferred out of the conductor contributed to protecting the coil. Dissipation of this energy in the plates would reduce the hot-spot temperature of the conductor section which initiated a quench. The amount of reduction depends on the delay between the time the conductor goes normal and the time the dump starts. Lue's measurements (1987) of hot-spot temperature on this coil with pre-set delay times of 2 and 6 s indicated that 8 and 22 kJ, respectively, would be added to the initial normal zone if there were no inductive coupling to the shorted plates. These measurements also indicated that the plate did not absorb much Joule heating until some time after the coil dump was initiated; this is consistent with the poor thermal contact between the conductor and the plates described above.

CONCLUSIONS

The following conclusions can be drawn from our experience in testing the plate structure support of the WH LCT coil:

- Mechanical measurements on the conductor and the structural plates appeared to prove the usefulness of the distributed structure in eliminating large stress concentrations.
- Stress analysis and strain gauge instrumentation should be better coordinated. No definitive comparison between the strain measurements and the stress analysis was possible. It would also be wise to have fewer strain gauges located at a few strategic locations instead of a wealth of gauges that produce repetitive and sometimes confusing data.
- The unintentional shorting of the plates caused large eddy currents whenever the coil was rapidly discharged, extending the recool time to get ready for the next test. However, the shorted plates absorbed some of the coil energy and thus reduced the possible hot-spot temperature in the conductor. Hence, it is possible to use the plate as a secondary circuit to protect the coil.
- The high-voltage withstand capability of the force-cooled coil was demonstrated, despite the disadvantage of the present plate scheme that every turn of the conductor had to be insulated from the ground potential. The coil withstood a maximum dump voltage of 2.44 kV in the extended single-coil charge test.
- Not potting the conductor to the plates resulted in local stick-slip under mechanical loads and poor thermal contact between conductor and plates.
- Auxiliary cooling channels to remove heat (such as nuclear heating) from the conductor are most desirable for cable-in-conduit conductors with long hydraulic lengths. Separate cooling for the structure would be prudent.
- The manufacture of a long (4.7-km), helium-tight, stainless steel conduit for a force-cooled magnet has proved feasible even without a hermetic case.

REFERENCES

Beard, D. S., et al., editors (1988). The IEA Large Coil Task. Fusion Engineering and Design, Vol. 7, nos. 1 & 2, pp. 1–232.

Dresner, L., et al. (1987). First Tests of the Westinghouse Coil in the International Fusion Superconducting Magnet Test Facility. IEEE Transactions on Magnetics, Vol. MAG-23, pp. 1701–1705.

Dresner, L., et al. (1988). Stability Tests of the Westinghouse Coil in the International Fusion Superconducting Magnet Test Facility. IEEE Transactions on Magnetics, Vol. MAG-24, pp. 779–782.

Lue, J. W., et al. (1987). Hot-Spot Measurements on the US-LCT Coils in the IFSMTF. Proc. 12th Symp. on Fusion Engineering, Monterey, California, Vol. I, pp. 369–372.

Luton, J. N., et al. (1987). A Study of Eddy Current Effects in the Structure of the Westinghouse LCT Coil. IEEE Transactions on Magnetics, Vol. MAG-23, pp. 1497–1500.

Singh, S. K., et al. (1987a). Advantages of the Distributed Structure Concept of the Westinghouse LCP Coil Design-II. IEEE Transactions on Magnetics, Vol. MAG-23, pp. 1501–1504.

Singh, S. K., et al. (1987b). Manufacture of the Westinghouse Forced Flow Nb_3Sn Test Coil for the Large Coil Program. IEEE Transactions on Magnetics, Vol. MAG-24, pp. 1509–1512.